Ultra-fast bandgap photonics in mid-IR wavelengths

Enam Chowdhury*[a], Kyle R. P. Kafka[a], Drake R. Austin[a], Kevin Werner[a], Noah Talisa[a], Boquin Ma[b], Cosmin I. Blaga[a], Louis F. Dimauro[a], Hui Li[a], Allen Yi[a]
aThe Ohio State University, 191 W Woodruff Avenue, Columbus, OH; bCommunications University of China

ABSTRACT

Ultrafast bandgap photonics in mid-infrared is an exciting area of nonlinear photonics, which shows different ultrafast damage characteristics of solids compared to that in near-infrared fields. It allows periodic surface nano-structures formation in low bandgap materials like germanium. Ultrafast mid-infrared field interaction at 2 micron wavelength with non-linear photonic crystal results in generation of high efficiency harmonic generation upto sixth harmonic.

Keywords: mid-infrared, ultrafast interaction, laser induced damage, laser induced periodic surface structure, non-linear photonic crystal, high harmonic generation, ionization of solid, plasmonics.

1. INTRODUCTION

There has been a tremendous interest in studying femtosecond laser matter interaction in mid-infrared wavelength ranges, because of existence of many molecular resonances in 2-10 μm wavelength range [1], enhancement of electron ponderomotive energy at longer wavelengths due to λ^2 scale, efficient generation of XUV attosecond pulses [2], imaging and detection of cancer and many other applications [3]. Mid-IR (will be referred to as MIR henceforth) femtosecond interaction with solids are interesting in their own right for several reasons. For traditional insulators, the reduced individual photon energies at mid IR wavelengths should exhibit a transition from multiphoton to tunneling ionization, when compared to similar interactions with UV-VIS-near-IR femtosecond pulses. Semiconductors like Si and Ge become transparent 'high band gap' semiconductor at mid-IR wavelengths. With fluence near damage threshold, when sufficient electron population transfer into conduction band occurs and all insulators become metal-like, MIR frequencies present and interesting paradigm, i.e. much larger ponderomotive energies of electrons (compared with near-IR wavelengths) which may be very sensitive to alignment of laser polarization direction along different lattice axes of symmetry. Interaction of such excited electrons with lattice under strong MIR fields also led to high harmonic generation in solids, which will be discussed. As a multiple pulse laser matter interaction phenomenon, laser induced Periodic Surface Structures (LIPSS) formation from near-IR to MIR wavelengths generation will be discussed, as LIPSS carry great importance in laser micro/nano machining, surface modification applications such as solar cells, wave guides, super hydrophobic surfaces, integrated optoelectrnic and optoplasmonic devices and many others [4]. The exact process of LIPSS generation is not completely understood [5]. Dynamics of the process is studied by us from femtosecond to nanosecond regime to properly understand how short lived surface field ripples can guide material movements at much longer timescale.

1.1 New Paradigm

MIR fields also offer a new paradigm for intense laser solid interaction from various aspects, as shown in Table 1:

Table 1. Ultrafast laser solid dynamics parameters in MIR wavelengths slightly above damage threshold intensity of silicon. Mass of electrons, m_e is assumed to be equal to its vacuum mass, for both U_p and n_c calculations.

Intensity 5 x 10^{12} W/cm^2, Silicon direct E_g = 3.4 eV				
Wavelength (nm)	Photon Energy (eV)	Keldysh param. $\Upsilon = \omega\sqrt{(2E_g)}/F$	Ponderomotive energy U_p (eV)	Critical Density n_c (cm^{-3})
400	3.1	2.8	0.07	7 10^{21}
800	1.55	1.38	0.29	1.7 10^{21}
2000	0.61	0.55	1.8	3 10^{20}
4000	0.31	0.28	7.3	7 10^{19}

*chowdhury.24@osu.edu; phone 1 614 247-8392; fax 1 614 292-7557; https://u.osu.edu/chowdhury.24/

Ultrafast Bandgap Photonics, edited by Michael K. Rafailov, Eric Mazur, Proc. of SPIE Vol. 9835, 983519 · © 2016 SPIE
CCC code: 0277-786X/16/$18 · doi: 10.1117/12.2223481

At an intensity just above femtosecond laser induced damage threshold (LIDT) in Si [6], turning the laser wavelength knob to MIR affects ionization, electron dynamics and plasmon coupling simultaneously. Ionization/transition from valence to conduction band mechanism tend to shift from purely multi-photon, to tunneling regime (true for direct bandgap of 3.4 eV as well), as observed with the change in Keldysh parameter γ. Since the generation of 'free' electrons in solids affects many mechanisms from free carrier absorption (FCA), laser damage, supercontinuum generation to high harmonic generation, understanding photo-ionization mechanism becomes the first step in understanding all the ultrafast bandgap photonics (UBG) effects. The fourth column of Table 1 shows that once electrons are in the conduction band, they would gain cycle average energy (ponderomotive energy, PE) in the laser field, which is proportional to λ^2, and inversely proportional to electron effective mass, which shows that even for moderate intensities, at longer wavelengths, in materials with small optical effective mass (e.g. Si and Ge), electrons in conduction band will rapidly attain enough PE to overcome electron affinity and be free. This situation opens up to create additional complexity for laser material interaction at oblique incidence with s and p polarization, where s polarization field excites electrons inside surface, in the case of p-polarization, a strong E field component exists normal to the surface to pull electrons out of solid and back into it, resembling vaccum/Brunel heating at ultrahigh intensities. Once the electrons are out of the solid, their effective mass is no longer dressed by crystal potentials, and this transition of electron effective mass at the boundary provides another complication in studying UBG effects at longer wavelengths. Finally, the fifth column describes how plasma critical density, proportional to m_{eff}/λ^2, changes for longer wavelengths, which would allow plasmon coupling in longer wavelength [7] with high doping alone (e.g. in Ge). Plasmon coupling allows light fields to be coupled to subwavelength structures, micro-electronic circuits directly, and could be a gamechanger for Lab-on-a-chip type architecture for long wavelength applications [8].

1.2 Experimental Challenges

Strong field MIR studies pose unique challenges for an experimental program, as sources are still in developmental stages, optics, beam alignment and characterization tools are in their early stage, and very expensive. For example, traditional IR cards do not work beyond 1.7 um wavelength, camera prices range from $10 k - $70 k (whereas for NIR, even < $10 webcam works), photodiodes, spectrometers etc. are also much more expensive than the VIS-NIR counterparts. High reflectors and high efficiency polarizers are also difficult to manufacture due to large λ/4 layer thickness.

2. MIR MULTI-PULSE EFFECTS

2.1 Multi-pulse damage

Fig. 1 shows the measured LIDT at 3600 nm wavelength for 45 degree angle of incidence at *p*-polarization, as a function of pulse number for Ge, Si, sapphire, and CaF_2, denoted by F(*N*), where *N* is the pulse number. LIDT values for sapphire and CaF_2 could not be determined with less than 100 pulses due to limitations in the available pulse energy. All materials show a decreasing trend with the number of pulses, with Si and Ge converging to a constant value F(∞) after approximately 1000 pulses. This has been attributed to the accumulation of defects that allow for additional excitation with subsequent

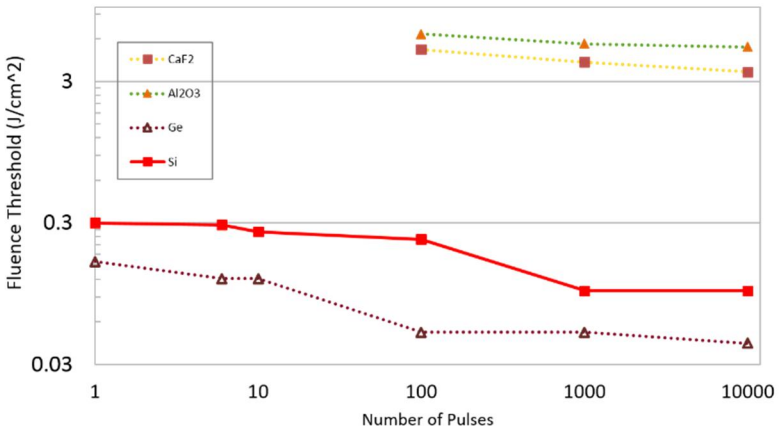

Figure 1 MIR multi-pulse damage threshold of different materials for 90 fs, 3600 nm pulses.

laser shots [9], [10]. Sapphire and CaF_2, however, continue to exhibit a decrease in LIDT even at $F(10^4)$, whereas in previous works with Near IR pulses [11], multi-pulse damage fluence reach saturation around > F(100). This can possibly be attributed to the formation of self-trapped excitons (STE), a type of defect known to form in wide-gap dielectrics [10], and also multiple deep and shallow traps with long life time. Very high ponderomotive energy available to conduction electrons in MIR multi-pulse interaction may also play a differentiating role, which has not been explored. What is also different from previous work is that whereas, Mero et al. reported $F(\infty)/F(1) = 0.67$ for large bandgap oxides for NIR multi-pulse damage thresholds, in MIR, we observe $F(\infty)/F(1) = 0.33$ for Si, and 0.25 for Ge for similar band gap and photon energy ratios in [10].

Additionally, the LIDT scales with the band-gap of the material, with the low band-gap semiconductors (0.67 and 1.12 eV for Ge and Si, respectively) exhibiting much lower LIDT compared to the dielectrics (9.9 and 12 eV for sapphire and CaF_2, respectively). This is because a sufficient conduction band electron density is needed in order for damage to occur, at which point the material will rapidly absorb laser energy [12]. In case of Si and Ge (especially Ge) ~10^{13} or larger free carriers already exist in room temperature, which do not need photo-induced transition into conduction band, but can instantaneously absorb laser energy, and allow collisional ionization to significantly add to electron density apart from photoionization. With a larger band-gap, free-carriers are negligible in undamaged sapphire or CaF_2, higher intensities are needed to achieve the same ionization rate because a greater number of photons are (30 and 37, respectively) needed to excite a single electron to the conduction band, rendering ionization process in the tunneling regime.

2.2 Laser Induced Periodic Surface Structures (LIPSS) in MIR

Femtosecond LIPSS is a single-step process of multiple femtosecond laser pulses interacting with solid surfaces that allows creation of ordered nano to micro structures on surfaces on virtually any materials, metals, insulators or semiconductors, have shown much promise in a wide range of applications, from super-hydrophobic surfaces to solar cells. Although LIPSS in CW/ns/fs regimes have been studied for over three decades, there has not been much efforts devoted to fs-MIR LIPSS formation [13]. The first systematic work on femtosecond MIR (beyond 2400 nm) LIPSS was reported by Austin et. al. [14] revealing the formation of both low (spatial period, $\Lambda \geq \lambda/2$) and high spatial frequency ($\Lambda < \lambda/2$) LIPSS (LSFL and HSFL, respectively) in germanium at 3000 and 3600 nm, generated by a KTA based 90 fs home-built optical parametric amplifier system (OPA) pumped by a kHz Ti:Sapphire system. Femtosecond MIR interaction can generate a wide range of periodic structures on semiconductors, as shown in Figures 2 and 3. Fig 2(a) shows various periodic structures formation on Ge, where central LSFL ($\Lambda \approx$ 2 um) formation is due to backward-propagating surface plasmon coupling with the incoming laser pulses, as explained in [14]. HSFL grooves parallel to laser polarization direction also formed in the periphery (period≈500 nm) after exposure to 3.6 um wavelength pulses. These are thought to form via a surface scattering process [15], where initial laser pulses roughen the surface, which then act as scatterers for next laser pulses. The scattered light along the surface interfere with the incoming light to create a spatially dependent field intensification pattern that can be expressed in terms of an efficacy factor $\eta(\mathbf{k})$ as a function of spatial frequency $\mathbf{k}$. The LIPSS spatial frequency typically is represented by peaks in the efficacy curve. Typically, the spatial wavelength of HSFL can be represented by following equations,

$$\Lambda = \frac{\lambda}{n \pm \sin\theta} \quad (1)$$

where eq. (1) represents interaction non-normal incidence angle where laser $\mathbf{k}_{||}$ (parallel to surface) and scattered wave vector are collinear, with angle of incidence θ, and n being the index of refraction of the material. With index of Ge being ~4 at MIR wavelengths, the HSFL frequency (~500 nm, $\lambda/\Lambda \sim 7.2$) doesn't match this simple analysis. It turns out that the index of refraction has to be modified due to the excited dielectric function of the solid interacting with the laser pulses, taking into account of the presence of free electrons, collisional contributions and Kerr effect as well. Still, only a class of HSFLs generated from MIR interactions can be explained this way. Fig. 2(b) shows HSFL ($\Lambda \approx$ 200 nm) perpendicular to laser polarization formed on Si with 800 nm wavelength pulses. However, such structures were not observed on silicon at MIR wavelengths, regardless of the fluence used. Instead, a series of thin grooves were observed to form parallel to the laser polarization (Fig. 3). After exposure to 100 pulses with a wavelength of 3.6 um, these grooves were found to have a separation of approximately 700 nm. In addition, the width of these structures was found to be approximately 100 nm, substantially shorter than the short pulse wavelength (λ/36). These are one of the smallest sub-wavelength scale grooves ever observed. Efforts are under way to analyze how these grooves form, and whether they are influenced by orientation of Si crystal with respect to the laser polarization or not.

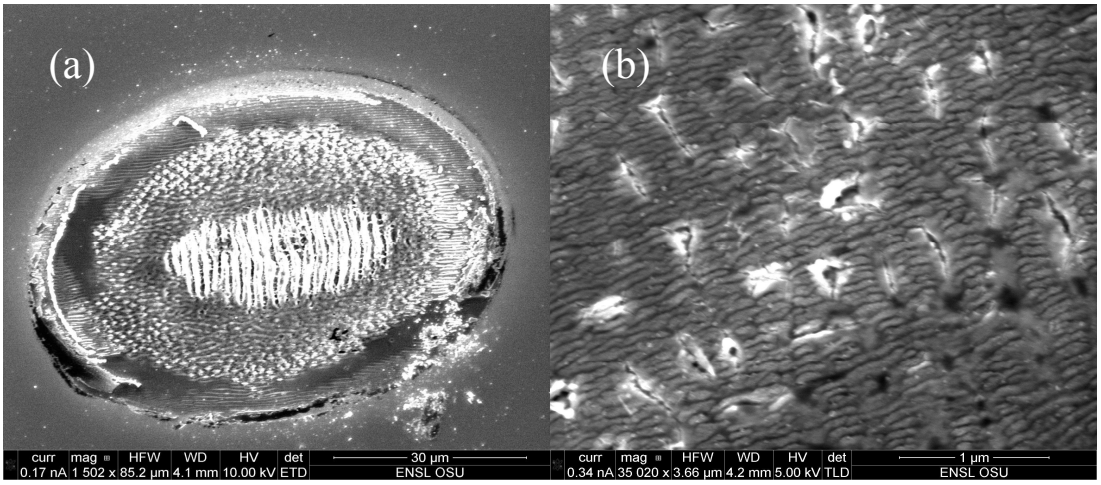

Figure 2 (a) MIR femtosecond laser pulse induced periodic structures on Ge, generated by 1000 pulses with 90 fs pulsewidth incident at 45 degree with *p*-polarization at 3600 nm wavelength, with ~4J/cm^2 fluence. LSFL formation seen is oriented perpendicular to laser polarization. (b) HSFL generation on Si with 1000 NIR laser pulses at 1 J/cm^2 fluence with 800 nm, 30 fs at 45 degree angle of incidence with *p*-polarization. HSFL orientation is perpendicular to laser polarization.

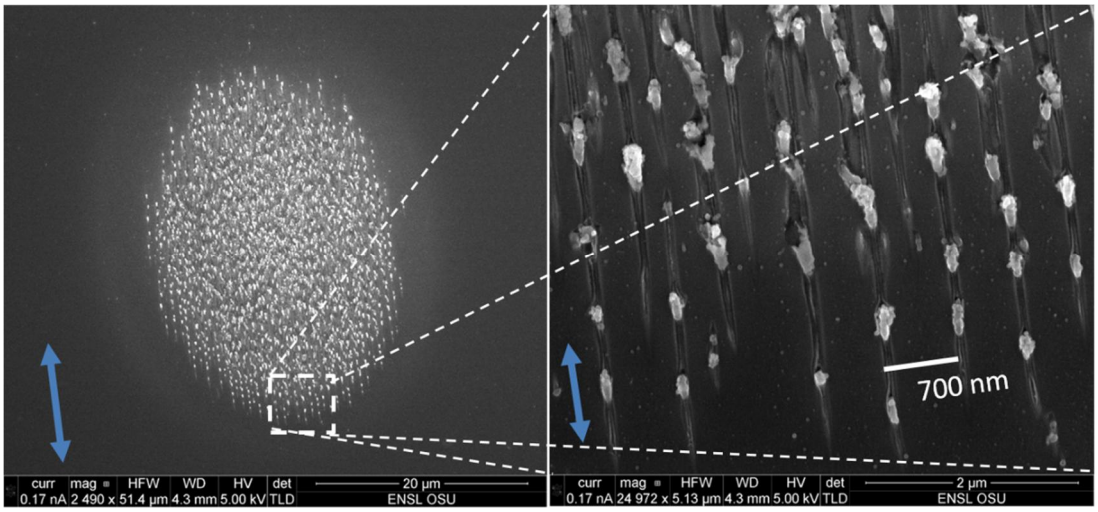

Figure 3 MIR femtosecond sub-wavelength structure formation in Si. Figure on right shows a magnified region wtih 100 nm trench-like formation generated from 1000 pulses at 0.5 J/cm2 fluence at 3600 nm wavelength.

3. HHG FROM MIR INTERACTION WITH PHOTONIC CRYSTALS

Photonic crystals such as periodically-poled lithium-niobate (PPLN) are known to have the ability to generate nonlinear conversion through quasi-phase-matching [16], but by deviating from a simple 1-D periodic poling allowed us to experimentally simultaneously generate harmonics up to 6th order. Specifically, we used a LN crystal with a 2-D fractal superlattice poling structure [17], where the idea behind the fractal geometry was to create a poling pattern with geometric order/symmetry, while simultaneously expanding the number of spectral pathways for harmonic conversion. Femtosecond pulses at 2.05 um central wavelength were weakly focused ($2w_0$~200um, ~90fs, ≤40 uJ) into the crystal along the plane of its 2-D lattice, and a spectrum of harmonics from 2nd-6th were generated. The lack of harmonics beyond the 6th harmonic is likely due to single-photon absorption the 7th harmonic, for which the photon energy exceeds the intrinsic bandgap of LN.

The harmonics from this interaction formed a very complex beam structure, and the Fig. 4 shows the visual appearance of the beam incident upon a white piece of paper. The large angular divergence in the horizontal plane arises from the varied non-collinear harmonic pathways available from the 2-D lattice structure, and in this broad divergence one can discern

several peaks other than the central bright peak. In principle, a different 2-D lattice could be designed which engineers specific harmonics to be generated simultaneously along particular directions.

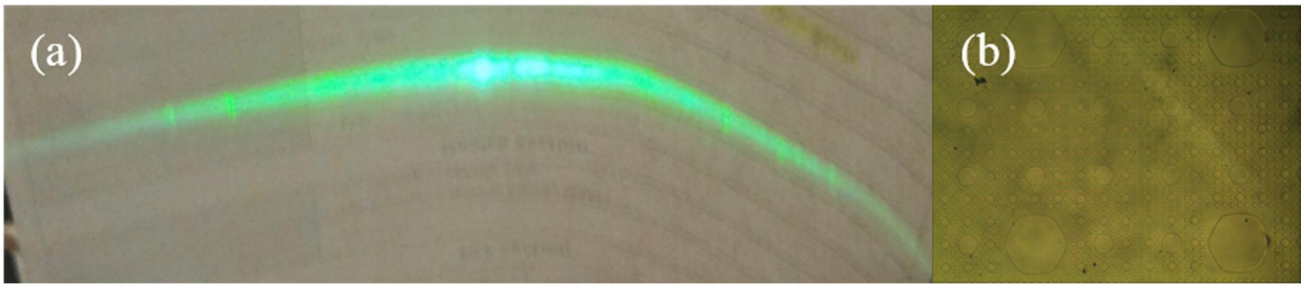

Figure 4 (a) Visual appearance of the beam of generated harmonics incident upon a (curved) white piece of paper. The greenish-blue dominant appearance is consistent with the 4th harmonic (510 nm), while other harmonics are on the edge or outside of the visible spectrum (2.05 um, 1.02 um, 0.68 um, 0.41 um, 0.34 um). (b) The Sierpinski super-lattice structure of the NPC under a microscope.

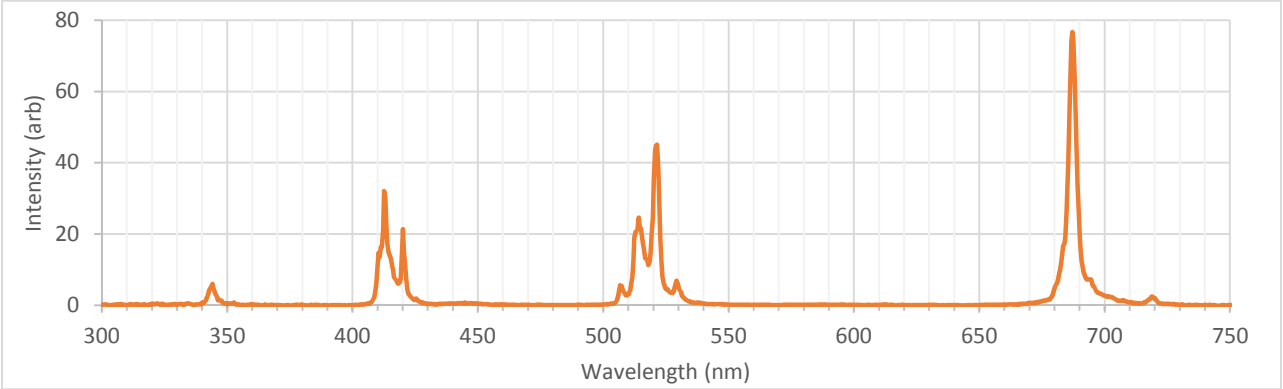

Figure 5 Spectrum of harmonics 3-6. The multi-peaked structure of the 4th and 5th harmonics is due to the presence of multiple nonlinear conversion pathways available within the bandwidth of the harmonic.

Conversion efficiency was measured by using a concave metal mirror to collect the total output harmonics onto an energy meter, then a series of spectral filters and spectrometers was used to measure the relative efficiencies. This resulted in a total harmonic yield of at least 11%, and as high as 16% for non-saturating fundamental intensities. An example spectrum of harmonics 3-6 is shown in Fig.5.

4. SUMMARY

In summary, strong field MIR interaction with regular and engineered solids provides an exciting new paradigm for non-linear optics and photonics, which can potentially be used in a large range of applications. When compared to strong field near-IR solid interaction, these interactions may induce traditional low bandgap materials to behave like high bandgap material with a significant free carrier density, modify interband transition from multi-photon into tunneling regime, and change the surface electron dynamics to usher in novel surface engineering avenues. Strong MIR fields applied to non-linear photonic crystals would allow creation of high harmonics from MIR to visible with tailor made angular emission and high efficiency for wide ranging appications in future.

5. ACKNOWLEDGMENT

This work was supported by the Air Force Office of Scientific Research (AFOSR), USA under grant no. FA9550-12-1-0454, FA9550-12-1-0047, and FA9550-16-1-0069 as well as the Air Force Research Laboratory, USA grant no. FA-9451-14-1-0351. The DiMauro group acknowledges support from MIR MURI grant FA9550-16-1-0013. C. I. Blaga acknowledges support from AFOSR YIP, grant FA9550-15-1-0203.

REFERENCES

[1] H. Pires, M. Baudisch, D. Sanchez, M. Hemmer, and J. Biegert, "Ultrashort pulse generation in the mid-IR," *Prog. Quantum Electron.*, vol. 43, pp. 1–30, 2015.

[2] T. Popmintchev, M.-C. Chen, D. Popmintchev, P. Arpin, S. Brown, S. Alisauskas, G. Andriukaitis, T. Balciunas, O. D. Mücke, A. Pugzlys, A. Baltuska, B. Shim, S. E. Schrauth, A. Gaeta, C. Hernández-García, L. Plaja, A. Becker, A. Jaron-Becker, M. M. Murnane, and H. C. Kapteyn, "Bright coherent ultrahigh harmonics in the keV x-ray regime from mid-infrared femtosecond lasers.," *Science*, vol. 336, no. 6086, pp. 1287–91, Jun. 2012.

[3] T. W. Neely, L. Nugent-Glandorf, and S. Diddams, "Broadband Mid-IR Standoff Spectroscopy of Explosives with a Femtosecond Optical Parametric Oscillator," *Lasers, Sources, Relat. Photonic Devices*, vol. 2, p. LT2B.3, 2012.

[4] A. Y. Vorobyev and C. Guo, "Direct femtosecond laser surface nano/microstructuring and its applications," *Laser Photon. Rev.*, vol. 7, no. 3, pp. 385–407, 2013.

[5] O. Varlamova, C. Martens, M. Ratzke, and J. Reif, "Genesis of femtosecond-induced nanostructures on solid surfaces," *Appl. Opt.*, vol. 53, no. 31, p. 11, 2014.

[6] D. Austin, K. Kafka, C. Blaga, L. F. Dimauro, and E. a. Chowdhury, "Measurement of femtosecond laser damage thresholds at Mid IR wavelengths," in *Proceedings of SPIE 9237, Laser-Induced Damage in Optical Materials*, 2014, p. 92370V.

[7] A. Boltasseva and H. a Atwater, "Materials science. Low-loss plasmonic metamaterials.," *Science*, vol. 331, no. 6015, pp. 290–1, Jan. 2011.

[8] R. Soref, "Mid-infrared photonics in silicon and germanium," *Nat. Photonics*, vol. 4, no. 8, pp. 495–497, 2010.

[9] D. Ashkenasi, M. Lorenz, R. Stoian, and a Rosenfeld, "Surface damage threshold and sturcturing of dielectrics using femtosecond laser pulses: the role of incubation," *Appl. Surf. Sci.*, vol. 150, pp. 101–106, 1999.

[10] M. Mero, B. Clapp, J. C. Jasapara, W. . Rudolph, D. Ristau, K. Starke, J. Krüger, S. Martin, and W. Kautek, "On the damage behavior of dielectric films when illuminated with multiple femtosecond laser pulses," *Opt. Eng.*, vol. 44, no. 5, p. 051107, May 2005.

[11] A. Rosenfeld, M. Lorenz, R. Stoian, and D. Ashkenasi, "Ultrashort-laser-pulse damage threshold of transparent materials and the role of incubation," *Appl. Phys. A*, vol. 69, no. 1, pp. S373–S376.

[12] B. C. Stuart, M. D. Feit, S. Herman, a. M. Rubenchik, B. W. Shore, and M. D. Perry, "Nanosecond-to-femtosecond laser-induced breakdown in dielectrics," *Phys. Rev. B*, vol. 53, no. 4, pp. 1749–1761, Jan. 1996.

[13] a. Borowiec and H. K. Haugen, "Subwavelength ripple formation on the surfaces of compound semiconductors irradiated with femtosecond laser pulses," *Appl. Phys. Lett.*, vol. 82, no. 25, pp. 4462–4464, 2003.

[14] D. R. Austin, K. R. P. Kafka, S. Trendafilov, G. Shvets, H. Li, A. Y. Yi, U. B. Szafruga, Z. Wang, Y. H. Lai, C. I. Blaga, L. F. DiMauro, and E. a. Chowdhury, "Laser induced periodic surface structure formation in germanium by strong field mid IR laser solid interaction at oblique incidence," *Opt. Express*, vol. 23, no. 15, p. 19522, 2015.

[15] H. Van Driel, J. Sipe, and J. Young, "Laser-induced periodic surface structure on solids: a universal phenomenon," *Phys. Rev. Lett.*, vol. 49, no. 26, p. 1955, 1982.

[16] M. Soljačić and J. D. Joannopoulos, "Enhancement of nonlinear effects using photonic crystals," *Nat. Mater.*, vol. 3, no. 4, pp. 211–219, 2004.

[17] B. Ma, B. Chen, R. Liu, and Z. Li, "Multiple shape light sources generated in $LiNbO_3$ nonlinear photonic crystals with Sierpinski fractal superlattices," *J. Opt.*, vol. 17, no. 8, p. 085503, 2015.